Rare Met. (2024) 43(4):1786–1792
https://doi.org/10.1007/s12598-019-01276-5

RARE METALS
www.editorialmanager.com/rmet

Microstructure and properties of coarse-grained WC–10Co cemented carbides with different carbon contents during heat treatments

Yuan-Feng Xie, Xing-Cheng Xie*, Zhong-Wu Li, Rui-Jun Cao, Zhong-Kun Lin, Qing Li, Chen-Guang Lin

Received: 4 February 2018 / Revised: 5 May 2018 / Accepted: 9 April 2019 / Published online: 11 July 2019

Abstract The effects of cryogenic treatment (CT) and tempering-cryogenic treatment (TCT) on the microstructure and properties of coarse-grained WC–10Co cemented carbides with different carbon contents were researched. The binder phase, WC mean grain sizes, W solubility in the binder, relative magnetic saturation, densities, hardness, wear resistance and second phase precipitation of cemented carbides with different heat treatments were discussed. The results show that there are significant changes of microstructure and properties in the samples with CT and TCT, especially due to the precipitation of metastable nanoparticles $W_xCo_yC_z$ in the binder during the heat treatments of CT and TCT. With the simultaneous combination of microstructure and nanoparticle-reinforced binder, a dramatically improved combination of hardness and wear resistance of the samples after TCT has been achieved.

Keywords Cryogenic treatment; Tempering; Coarse-grained cemented carbide; Carbon content; Nanoparticle-reinforced binder

1 Introduction

Coarse-grained WC–Co cemented carbides with the combination of high hardness, high strength and high wear resistance are quite widely used in gas and oil drilling, mining, rolling and construction [1–5]. The mechanical properties of cemented carbides are very sensitive to differences in carbon content [6]. As to the low carbon content cemented carbides, it is easier to precipitate the second phase which is deleterious to the properties of alloys [7, 8].

In recent years, cemented carbides have been improved by changing the composition or the microstructure. Heat treatment is one of the most valid methods for improving the mechanical properties of the sintered alloys, especially for cryogenic treatment (CT) [9, 10]. Thakur et al. [11] noted that the post-treated (cryogenic treatment, controlled heating and oil quenching) carbide tools showed better wear resistance, hardness and surface finish. Xie et al. [12] observed that η phase improved the cemented carbides' hardness, and bending strength increased during CT. Kalsi et al. [13] deduced that controlled CT could be beneficial for the fineness, uniform distribution and densification of cobalt binder which gave the carbides better properties because of the formation of W_2C and Co_3W_3C secondary carbides precipitated in cobalt binder. Zhang et al. [14] worked on ultrafine-grained cemented carbides; the improvement in the mechanical properties could be due to the Co phase transformation.

As mentioned above, the increased performance of cemented carbides treated by post treatments is attributed to the precipitation of a second phase. It was observed that deep CT and tempering introduced physical changes only in cobalt binder [15–18]. Konyashin et al. [19–22] investigated the strengthening mechanism in details of hardmetals with nano-strengthened binder, and maintained that a dramatically increased combination of hardness, wear resistance, fracture toughness and strength of WC–Co cemented carbides was a result of the precipitation of nanoparticles coherent with the Co matrix, such as Co_2W_4C in α-Co, Co_3W in ε-Co.

The literatures are mostly about the contribution of tempering to the mechanical properties of the cement

Y.-F. Xie, X.-C. Xie*, Z.-W. Li, R.-J. Cao, Z.-K. Lin, Q. Li, C.-G. Lin
Powder Metallurgy and Special Materials Research Department, General Research Institute for Nonferrous Metals, Beijing 100088, China
e-mail: xxc1014@126.com

carbides [9–18, 23, 24], but there is more work to do. This paper describes the attempt to improve the mechanical properties of coarse-grained WC–10Co cemented carbides, especially for the alloys with various carbon contents. In order to understand the effects of CT and tempering-cryogenic treatment (TCT) on the microstructure and properties, the experimental results were discussed with respect to the binder phase, WC mean grain sizes, W solubility in the binder, relative magnetic saturation, densities, hardness, wear resistance and second phase precipitation.

2 Experimental

2.1 Materials

Four WC–10Co coarse-grained cemented carbides with different carbon contents were prepared from the mixtures of WC powder (Fisher particle size (FSSS), 20 μm) and Co powder. The mixtures were milled for 28 h in ethanol with 2% paraffin, dried at 80 °C in a vacuum drier, then compacted at 200 MPa into blocks with dimensions of Φ10 mm × 5 mm and 10 mm × 10 mm × 25 mm. The compacts were sintered at 1430 °C for 1 h in a dewax-vacuum sintering furnace. The untreated (UT) four samples were labeled by UT-1, UT-2, UT-3, UT-4, the compositions and properties the properties of which are shown in Table 1. The cryogenically treated samples were labeled as CT-1, CT-2, CT-3, CT-4. The tempering-cryogenic treated samples were labeled as TCT-1, TCT-2, TCT-3, TCT-4. Electrolytic corrosion of WC was performed in an electrolyte consisting of 3 wt% NaOH, 2 at% $C_4H_6O_6$, 4 mol·L^{-1} $HClO_4$ by using a TPR-6410D potentiostat [25].

2.2 Heat treatment

The samples were treated with cryogenic treatments and tempering-cryogenic treatments. In the tempering treatment, the sintered samples were heated to 550 °C in the vacuum heat treatment furnace, and then held for 30 min and furnace cooled. During the cryogenic treatment, the samples were cooled in liquid nitrogen at a speed of 4 °C·min^{-1} to − 196 °C, then held for 2 h, and brought back to room temperature in the air.

2.3 Microstructure and properties analysis

The microstructures were investigated by using a JEOL SEM7001F field emission scan electronic microscope (FESEM) with a energy dispersive X-ray analysis (EDAX) and a JEOL JEF-2001F field emission high-resolution transmission electron microscope (HRTEM). X-ray diffraction (XRD) pattern was obtained using an X′ Pert PRO MPO type X-ray diffractometer. The measurement of mean grain size and grain contiguity was carried out by the linear intercept method using SEM and areas of more than 400 grains. The densities of the samples were obtained by the Archimedes' method using an analytical balance AL204. The hardness (HV_{30}) measurements were carried out according to VTD552 at a load of 298 N. The cobalt magnetism performance was obtained by a MCOM-III cobalt magnetism meter. The impact abrasive wear performance was measured by MLD-10-type dynamic load abrasive wear testing machine.

3 Results and discussion

3.1 Microstructure and phase composition

Figure 1 shows XRD patterns of four WC–10Co alloys with different carbon contents after electrolytic corrosion and different heat treatments. It reveals that there are both α-Co and ε-Co phases in CT-4 and TCT-3, which proves that the samples with low carbon content experience the phase transformation of Co under the cryogenic treatment. During the heating in sintering, there is phase transformation from ε-Co to α-Co; in contrast, α-Co to ε-Co happens during the cooling. The α-Co (fcc) is stable above 417 °C, and the ε-Co (hcp) is detrimental to the ductility

Table 1 Compositions and properties of untreated four WC–10Co cemented carbides

Samples	UT-1	UT-2	UT-3	UT-4
WC content/wt%	90	90	90	90
Co content/wt%	10	10	10	10
W/(WC + Co) content/wt%	0	0.625	1.875	3.125
Grain size/μm	3.6	3.1	2.7	2.4
Grain contiguity	0.38	0.40	0.34	0.33
Total carbon content/wt%	6.08	6.01	5.97	5.94
Density/(g·cm^{-3})	14.42	14.46	14.51	14.53
Targeted phases	WC + γ	WC + γ	WC + γ + η	WC + γ + η

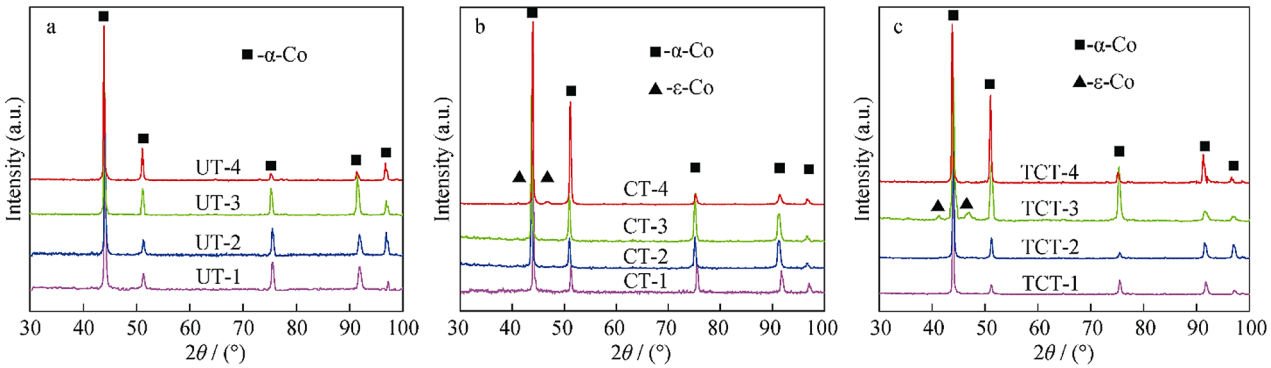

Fig. 1 XRD patterns of four WC–10Co alloys with different carbon contents after electrolytic corrosion and different heat treatments: **a** UT samples, **b** CT samples, and **c** TCT samples

stabilization below 417 °C [14]. There was no ε-Co in UT samples because the W and C atoms cannot precipitate from Co phase at high temperature [26]. Under low temperature, there is a greater two-phase free energy difference in the samples with lower carbon content, which promotes the trend of Co phase transformation [27].

In order to further study the martensite phase transformation of Co phase, energy-dispersive spectroscopy (EDS) analysis of W content in the Co was carried out, as shown in Fig. 2. Here, W solubility in Co binder of CT and TCT-3 and TCT-4 samples which mostly have α-Co → ε-Co transformation is notably higher than that of UT samples. However, when WC particles dissolve in α-Co phase, they not only reduce the possible ε-Co nucleation particles and improve the stacking fault energy, but also keep α-Co phase stable by the pinning effect of WC particles on the grain boundaries of the Co phase [14, 26]. Thus, it is a possible explanation that the transformation driving force of CT and TCT samples, which caused by two-phase free energy difference, is more than the preventing force caused by W solubility in Co phase; in other words, the transformed amount of ε-Co phase is increased. In addition, high W solubility is helpful for η phase precipitation. Therefore, CT-3, CT-4, TCT-3 and TCT-4 samples with high W solubility in the binder tend to precipitate the η phase.

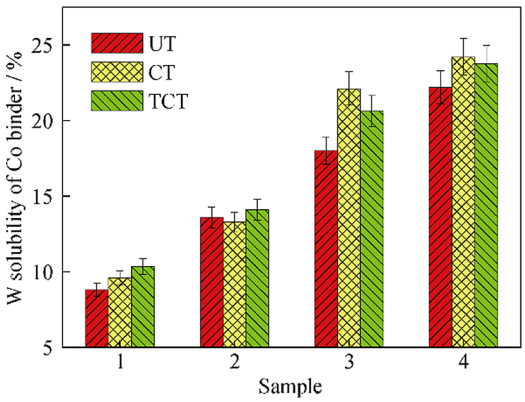

Fig. 2 W solubility of Co binder of four WC–10Co alloys with different carbon contents after different heat treatments

Figure 3 and Table 2 show the microstructures and WC mean grain sizes of four WC–10Co alloys with different carbon contents after different heat treatments (UT, CT and TCT). After various heat treatments, the WC grains with no noticeable difference in grain size are stable and stoichiometric. Thus, as the carbon contents of CT and TCT samples decrease, the WC mean grain sizes decrease, which is consistent with those of UT samples. WC grains with uneven angular shapes are found in the microstructures of UT samples (Fig. 3a, d, g, j). WC grains of CT (Fig. 3b, e, h, k) and TCT (Fig. 3c, f, i, l) samples tend to be smooth, due to the partial disappearance of sharp angles, especially for the CT-4 (2.6 μm) and TCT-4 (2.5 μm) samples whose grain contiguity are both slightly larger than that of UT-4 sample (2.4 μm), which is in good agreement with the results by Gill et al. [28]. In addition, there is a slight increase for WC mean grain sizes in CT samples and a slight decrease in TCT ones, as shown in Fig. 3 and Table 2. The change of WC mean grain sizes can be caused by the activation energy which is sensitive to carbon content. Thus, both η-phase and carbon self-diffusion at the interface between WC and Co phases affect the coarsening and refining of WC grains [29, 30]. Xie et al. [12] reported that cobalt densification has a definite effect on WC coarsening during cryogenic treatment, because cobalt densification plays the role of catalyst for growth of three of the six prismatic WC planes [31]. However, both Thakur et al. [11] and Kalsi et al. [13] only confirmed that cobalt densification improved the microhardness and wear resistance by cryogenic treatment. Therefore, to confirm the effect of cobalt densification on the WC coarsening, more evidence is needed.

3.2 Properties

Figure 4 shows the relative magnetic saturation of four WC–10Co alloys with different carbon contents after

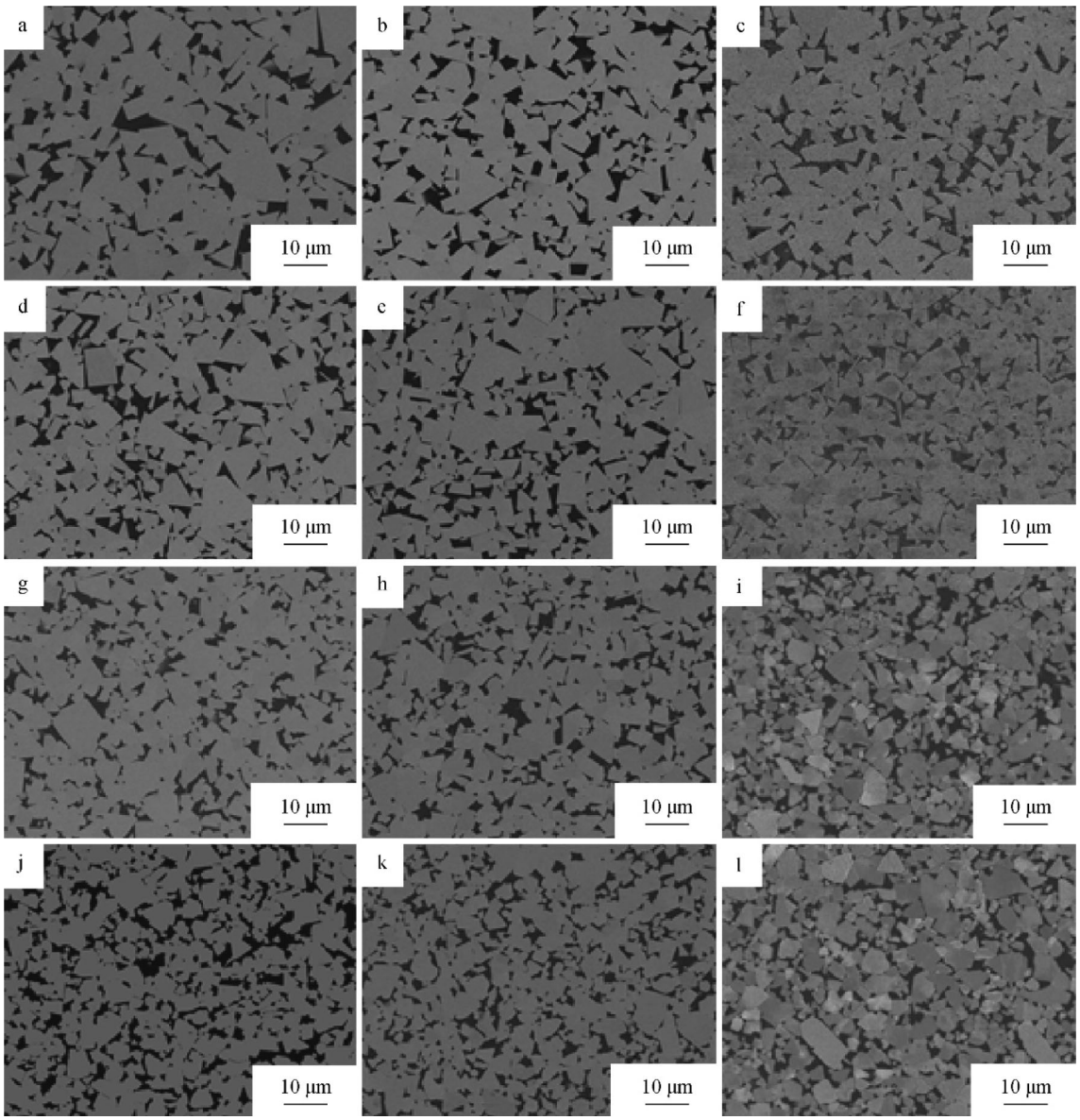

Fig. 3 Backscattered electron (BSE) images of four WC–10Co alloys with different carbon contents after different heat treatments: **a** UT-1, **b** CT-1, **c** TCT-1, **d** UT-2, **e** CT-2, **f** TCT-2, **g** UT-3, **h** CT-3, **i** TCT-3, **j** UT-4, **k** CT-4, and **l** TCT-4

Table 2 WC mean grain sizes of four WC–10Co alloys with different carbon contents after different heat treatments (μm)

Samples	UT	CT	TCT
1	3.6 ± 0.3	3.8 ± 0.4	3.4 ± 0.3
2	3.1 ± 0.3	3.1 ± 0.2	2.9 ± 0.2
3	2.7 ± 0.2	2.9 ± 0.2	2.4 ± 0.2
4	2.4 ± 0.2	2.6 ± 0.2	2.5 ± 0.2

different heat treatments. The relative magnetic saturation is related with carbon content and W solution in cobalt [12]. The lower the carbon content is, the smaller the relative magnetic saturation is; the higher the W solubility is in cobalt, the smaller the relative magnetic saturation is. As seen from Figs. 2, 4, as the relative magnetic saturation of CT and TCT samples decreases, cryogenic treatment further promotes W solution in cobalt. For the alloy with low carbon content, W solution is beneficial for the precipitation of η phase in γ phase [26]. Thus, cryogenic treatment is beneficial for the samples with lower carbon content (CT-3, CT-4, TCT-3 and TCT-4) to be with the precipitation of η phase.

The densities of four WC–10Co alloys with different carbon contents after different heat treatments are shown in Table 3. The density is mainly dependent on WC, Co phase, η phase or graphite. It can be clearly seen from Table 3 that there is little change in the densities of WC–

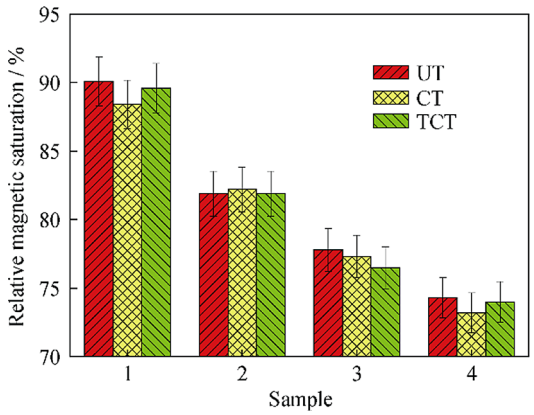

Fig. 4 Relative magnetic saturation of four WC–10Co alloys with different carbon contents after different heat treatments

Table 3 Densities of four WC–10Co alloys with different carbon contents after different heat treatments ($g \cdot cm^{-3}$)

Samples	UT	CT	TCT
1	14.42	14.40	14.40
2	14.46	14.48	14.46
3	14.51	14.50	14.52
4	14.53	14.52	14.53

10Co samples. Combined with Fig. 3, there is no micrometer-sized η phase and no noticeable porosity. So cryogenic treatment makes no effect on the densities of WC–10Co samples with different carbon contents. However, as Fig. 2 shows, as the carbon content decreases, there is more W dissolved in cobalt in the three-phase (WC + γ + η) of Samples 3 and 4. Thus, the densities of Samples 3 and 4 should increase. Thus, there are fewer or smaller-sized η phase precipitated in the cobalt phase.

Figure 5 shows the hardness of four WC–10Co alloys with different carbon contents after different heat treatments. According to classical Hall–Petch relationship [32] and WC mean grain sizes (Table 2), the hardness of UT samples should have been lower than that of TCT samples, but higher than that of CT samples, which is in good agreement with the experimental results shown in Fig. 5. The increased hardness is due to compressive residual stress and densification of Co phase during the cryogenic treatment. The Co phase transformation is too weak to affect the hardness during the cryogenic treatment [27]. According to Konyashin et al. [19–22], nano η phase could cause the dispersion strengthening of the Co phase. Thus, the improved hardness of the alloys after TCT should be due to the formation of the η phase.

Figure 6 shows wear resistance of four WC–10Co alloys with different carbon contents after different heat treatments. As the wear time increases, the wear loss increases; as the carbon content decreases, the wear loss decreases. After dynamic wearing for 2.5 h, the wear coefficients of samples with CT and TCT are lower than those of UT. Thus, CT and TCT improve the impact abrasion resistance; however, the samples after TCT have the best wear performance. According to the impact abrasive wear mechanisms [1, 2, 33], Co phase is removed and peels off until WC grain particles are separated and fall off. The WC phase is subjected to compressive stress and the binder to tensile stress [11]. After the heat treatments of CT and TCT, the residual stress decreases [27] and the compressive stress increases, which is beneficial for preventing the WC fracturing and detaching. Additionally, traditional η phase is helpful for improving the hardness and wear resistance of the low carbon content cemented carbide [34]. Thus, it is mostly assumed that η phase is precipitated in the cobalt phase during the heat treatments.

3.3 η Phase

Based on above all these results and analysis mentioned, there is possible η phase in Samples 3 and 4, especially for

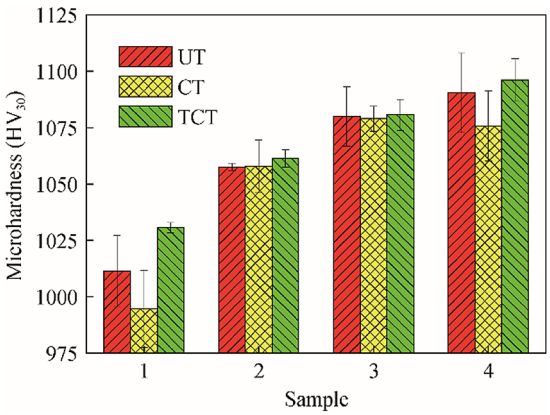

Fig. 5 Hardness of four WC–10Co alloys with different carbon contents after different heat treatments

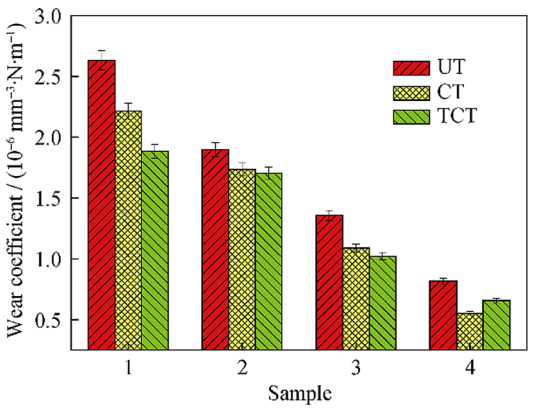

Fig. 6 Wear coefficients of four WC–10Co alloys with different carbon contents after different heat treatments

CT-3, CT-4, TCT-3 and TCT-4. Thus, further research on η phase in Sample TCT-4 with better mechanical properties was conducted. Figure 7 shows the structure of the binder in TCT-4 and UT-4 samples. As seen from Fig. 7a, there is less carbon content and some tungsten dissolved in the binder. For the cemented carbides with lower carbon content, it is possible to form $W_xCo_yC_z$ including Co_3W (hcp), Co_3W_3C (fcc), Co_2W_4C (fcc) and Co_6W_6C (fcc) during sintering [11, 19–23]. Combined with Fig. 2, W solubility in the binder of the sample with CT and TCT is quite high. Thus, CT and TCT may lead to the precipitation of nanoparticles in γ phase. Compared with UT-4 (Fig. 7d), it can be seen from HRTEM images (Fig. 7b, c) on (111) lattice plane that nanoparticles with about 5 nm in size are precipitated in α-Co phase. Because of fcc structure of α-Co matrix and difference in lattice constants, $W_xCo_yC_z$ nanoparticles with fcc structure grown in the matrix by the formation of low energy coherent or semi-coherent interface are mostly metastable, which is in good agreement with the results by Konyashin et al. [19]. Konyashin et al. [20] showed that the microhardness of nano-strengthened cobalt was higher than that without nano-strengthening. Therefore, η phase has great effect on the microstructure and properties of the samples with CT and TCT by the solid solution strengthening.

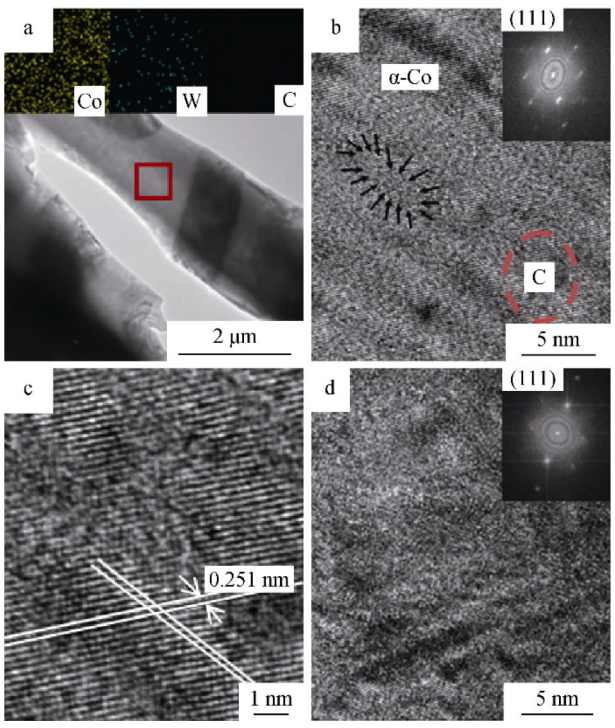

Fig. 7 Structure of binder in samples: **a** TEM image of alloy and inserted EDAX area-scanning images of red rectangular area showing contributions of Co, W and C (TCT-4); **b** HRTEM image of binder and inserted faster Fourier transformation (FFT) pattern (TCT-4); **c** HRTEM image of area indicated by red ellipse shown in **b** (TCT-4); **d** HRTEM image of binder and inserted FFT pattern (UT-4)

4 Conclusion

In this study, the effects of cryogenic treatment (CT) and tempering-cryogenic treatment (TCT) on the microstructure and properties of coarse-grained WC–10Co samples with different carbon contents were investigated. The CT and TCT heat treatments play an important role in affecting the microstructure and the nanoparticle-reinforced binder of the samples with lower carbon contents. There was phase transformation from ε-Co to α-Co, change of WC mean grain sizes, higher W solubility in the binder, and higher hardness and wear resistance in the CT and TCT samples. In particular, the precipitation of metastable nanoparticles $W_xCo_yC_z$ in the binder greatly improved the hardness and wear resistance of the samples after TCT.

Acknowledgements This work was financially supported by the General Research Institute for Nonferrous Metals Youth Science Foundation (No. 52147).

References

[1] Beste U, Jacobson S. A new view of the deterioration and wear of WC/Co cemented carbide rock drill buttons. Wear. 2008; 264(11–12):1129.
[2] Beste U, Jacobson S, Hogmark S. Rock penetration into cemented carbide drill buttons during rock drilling. Wear. 2008; 264(11–12):1142.
[3] Konyashin I, Straumal BB, Ries B, Bulatov MF, Kolesnikova KI. Contact angles of WC/WC grain boundaries with binder in cemented carbides with various carbon content. Mater Lett. 2017;196:1.
[4] Cao RJ, Lin CG, Xie XC, Lin ZK. Microstructure and mechanical properties of WC–Co-based cemented carbide with bimodal WC grain size distribution. Rare Met. 2018. https://doi.org/10.1007/s12598-018-1025-y.
[5] Zhang WB, Liu XZ, Chen ZH. Latest development of WC–Co cemented carbide. Chin J Rare Met. 2015;39(2):178.
[6] Bose A. A perspective on the earliest commercial PM metal-ceramic composite: cemented tungsten carbide. Int J Powder Metall. 2011;47(2):31.
[7] Ishida M, Hayashi K. Properties of WC–17 mass% Co cemented carbides with extremely low carbon contents. J Jpn Soc Powder Metall. 1995;42(4):427.
[8] Suzuki H, Tanase T, Nakayama F. Strength decrease in WC–Co low carbon cemented carbide due to precipitation treatment. J Jpn Soc Powder Metall. 1976;23(5):163.
[9] Cheng X, Zhang L. Effects of heat treatment on the mechanical properties of coarse-grained cemented carbide. Rare Met Cem Carbides. 2012;40(2):45.
[10] Celik ON, Sert A, Gasan H, Ulutan M. Effect of cryogenic treatment on the microstructure and the wear behavior of WC–Co end mills for machining of Ti6Al4V titanium alloy. Int J Adv Manuf Technol. 2018;95(5–8):2989.

[11] Thakur DG, Ramamoorthy B, Vijayaraghavan L. Effect of posttreatments on the performance of tungsten carbide (K20) tool while machining (turning) of Inconel 718. Int J Adv Manuf Technol. 2015;76(1–4):587.
[12] Xie CH, Huang JW, Tang YF, Gu LN. Effects of deep cryogenic treatment on microstructure and properties of WC–11Co cemented carbides with various carbon contents. Trans Nonferrous Met Soc China. 2015;25(9):3023.
[13] Kalsi NS, Sehgal R, Sharma VS. Comparative study to analyze the effect of tempering during cryogenic treatment of tungsten carbide tools in turning. Adv Mater Res. 2012;410:267.
[14] Zhang HJ, Chen LQ, Sun J, Wang WG, Wang QZ. Influence of deep cryogenic treatment on microstructures and mechanical properties of an ultrafine-grained WC–12Co cemented carbide. Acta Metall Sin (Engl Lett). 2014;27(5):894.
[15] Stewart HA. Cryogenic treatment of tungsten carbide reduces tool wear when machining medium density fiberboard. For Prod J. 2004;54(2):53.
[16] Steward H. A look at cryogenic treatment of tool metals. FDM ABI/INFORM Glob. 2008;80(1):64.
[17] Gallagher AH, Agosti CD, Roth JT. Effect of cryogenic treatments on tungsten carbide tool life: microstructural analysis. Trans North Am Manuf Res Inst SME. 2005;33:153.
[18] Padmakumar M, Dinakaran D, Guruprasath J. Characterization of cryogenically treated cemented carbide. Integr Ferroelectr. 2017;185(1):65.
[19] Konyashin I, Lachmann F, Ries B, Mazilkin AA, Straumal BB, Kübel C, Llanes L, Baretzky B. Strengthening zones in the Co matrix of WC–Co cemented carbides. Scr Mater. 2014;83:17.
[20] Konyashin I, Ries B, Lachmann F, Mazilkin AA, Straumal BB. Novel hardmetal with nano-strengthened binder. Inorg Mater. 2011;2(1):19.
[21] Konyashin I, Ries B, Lachmann F, Cooper R, Mazilkin A, Straumal B, Aretz A, Babaev V. Hardmetals with nanograin reinforced binder: binder fine structure and hardness. Int J Refract Met Hard Mater. 2008;26(6):583.
[22] Konyashin I, Ries B, Hlawatschek S, Mazilkin A. Novel industrial hardmetals for mining, construction and wear applications. Int J Refract Met Hard Mater. 2018;71:357.
[23] Kalsi NS, Sehgal R, Sharma VS. Effect of tempering after cryogenic treatment of tungsten carbide-cobalt bounded inserts. Bull Mater Sci. 2014;37(2):327.
[24] Yang HS, Wang J, Shen BL, Liu HH. Effect of cryogenic treatment on the matrix structure and abrasion resistance of white cast iron subjected to destabilization treatment. Wear. 2006;261(10):1150.
[25] Li ZW, Lin CG, Xie XC, Cao RJ, Lin ZK. Selective electrolytic corrosion behaviours of WC in WC–Co cemented carbide. Mater Sci Forum. 2017;898:1478.
[26] Liu SR, Liu Y. $\beta \rightarrow \alpha$ Transformation of γ-phase in sintered WC–Co cemented carbides. J Mater Sci Technol. 1996;12(5):398.
[27] Xie XC, Li ZW, Cao RJ, Lin ZK. Effects of heat treatments on the properties of coarse-grained WC–10Co cemented carbides with low carbon content. In: Sanya: Proceedings of the 14th Sino-Russia Symposium on Advanced Materials and Technologies; 2017. 93.
[28] Gill SS, Singh J, Singh H, Singh R. Metallurgical and mechanical characteristics of cryogenically treated tungsten carbide (WC–Co). Int J Adv Manuf Technol. 2012;58(1–4):119.
[29] Chivavibul P, Watanabe M, Kuroda S, Shinoda K. Effects of carbide size and Co content on the microstructure and mechanical properties of HVOF-sprayed WC–Co coatings. Surf Coat Technol. 2007;202(3):509.
[30] Borgh I, Hedström P, Borgenstam A, Ågren J, Odqvist J. Effect of carbon activity and powder particle size on WC grain coarsening during sintering of cemented carbides. Int J Refract Met Hard Mater. 2014;42:30.
[31] Konyashin I, Hlawatschek S, Ries B, Lachmann F, Dorn F, Sologubenko A, Weirich T. On the mechanism of WC coarsening in WC–Co hardmetals with various carbon contents. Int J Refract Met Hard Mater. 2009;27(2):234.
[32] Pande CS, Cooper KP. Nanomechanics of Hall–Petch relationship in nanocrystalline materials. Prog Mater Sci. 2009;54(6):689.
[33] Cao RJ, Lin CG, Ma XD, Xie XC, Lin ZK. Effect of cobalt content on wear behavior of coarse-grained hardmetals. Mater Sci Eng Powder Metall. 2015;20(6):860.
[34] Sun BQ, Wu GL, Zhou JH. η Phase in WC–Co alloy and its effect on property of the alloy. Cem Carbide. 1999;2:92.